



## Influence of developer and development conditions on the behavior of high molecular weight electron beam resists

D. G. Hasko, Shazia Yasin, and A. Mumtaz

Citation: *Journal of Vacuum Science & Technology B* **18**, 3441 (2000); doi: 10.1116/1.1319834

View online: <http://dx.doi.org/10.1116/1.1319834>

View Table of Contents: <http://scitation.aip.org/content/avs/journal/jvstb/18/6?ver=pdfcov>

Published by the AVS: Science & Technology of Materials, Interfaces, and Processing

---

### Articles you may be interested in

Selective profile transformation of electron-beam exposed multilevel resist structures based on a molecular weight dependent thermal reflow

*J. Vac. Sci. Technol. B* **29**, 06F302 (2011); 10.1116/1.3634013

Influence of molecular weight of resist polymers on surface roughness and line-edge roughness

*J. Vac. Sci. Technol. B* **22**, 2604 (2004); 10.1116/1.1805546

Effect of developer molecular size on roughness of dissolution front in electron-beam resist

*J. Vac. Sci. Technol. B* **22**, 1037 (2004); 10.1116/1.1736647

Polysubstituted derivatives of triphenylene as high resolution electron beam resists for nanolithography

*J. Vac. Sci. Technol. B* **18**, 2730 (2000); 10.1116/1.1322045

Nonstatistical degradation and development characteristics of poly(methylmethacrylate) based resists during electron beam exposure

*J. Vac. Sci. Technol. B* **16**, 2968 (1998); 10.1116/1.590327

---

## AVS 61<sup>ST</sup> INTERNATIONAL SYMPOSIUM & EXHIBITION

November 9-14, 2014 ⇄ Baltimore, Maryland

*Baltimore Convention Center*



# Influence of developer and development conditions on the behavior of high molecular weight electron beam resists

D. G. Hasko,<sup>a)</sup> Shazia Yasin, and A. Mumtaz

*Microelectronics Research Centre, Cavendish Laboratory, University of Cambridge, Madingley Road, Cambridge CB3 0HE, United Kingdom*

(Received 1 June 2000; accepted 25 August 2000)

The nature of the developer and development conditions of high molecular weight electron beam resists is known to influence sensitivity, contrast, line edge roughness, and ultimate resolution. These resist characteristics are explained using a dissolution model based on reptation theory and predictions are compared with experimental results on high molecular weight poly(methylmethacrylate) developed in a range of solvent mixtures and conditions, including ultrasonically assisted development. © 2000 American Vacuum Society.  
[S0734-211X(00)08806-5]

## I. INTRODUCTION

In order to predict resist pattern profiles with different development conditions in electron beam nanolithography, experimentally determined contrast curves, with large feature sizes, are used to determine the resist dissolution rate as a function of exposure dose. However, it is not clear that such dissolution rates are applicable to very small feature sizes. Moreover, recent experiments with a range of resists have shown improvements in lithographic behavior through the use of ultrasonically assisted development which cannot be explained using empirically determined contrast curves.<sup>1-3</sup> A physical model for the polymer dissolution process is needed to fully explain the ultimate resolution and line edge roughness behavior of electron beam resist.

The ultimate resolution of conventional electron beam resists, such as poly(methylmethacrylate) (PMMA), has been widely investigated, including the effects of developer, development conditions, such as ultrasonic agitation,<sup>4</sup> and polymer molecular weight.<sup>5</sup> In general, ultimate resolution is improved through the use of higher contrast developers, ultrasonic agitation, and through the use of high molecular weights. The use of membrane substrates to reduce the back-scattered electron contribution to the exposure has been found not to improve ultimate resolution, as first thought, but may improve the exposure dose latitude.<sup>5</sup> In the case of chemically amplified resists, the diffusion of the acid catalyst during the postexposure bake makes an additional contribution to the ultimate resolution;<sup>6</sup> we will not discuss this effect further. Despite the considerable experimental evidence, the mechanisms leading to an ultimate resolution remain unclear.

Previous investigations have attributed the origin of line edge roughness to aggregates in the resist film.<sup>7</sup> It was proposed that during development, aggregates in the resist film dissolved at a slower rate than the surrounding polymer matrix. As a result, the aggregate structure became exposed at the edges of features, so causing the edge roughness. The

measured size of the aggregates was found to correlate with the molecular weight of the resist used, being about 2–3 times the expected radius of gyration, however, the linewidth fluctuation was found to be independent of molecular weight.<sup>7</sup> This suggests that the origin of edge roughness was not in aggregates formed during the film casting process but in processes occurring during development.

The interaction of the polymer with the solvents in the developer, which controls the solubility and swelling of the resist, is central to understanding the nanolithographic behavior of a resist.<sup>8</sup> The interactions of PMMA with different solvents has been widely investigated,<sup>9</sup> especially with ketone-alcohol developer mixtures. Here, the ketone acts as a solvent and the alcohol as a nonsolvent, such solvent/nonsolvent combinations improve contrast and control of the development process. Polymer/solvent interactions also result in the free volume and dissolution properties of polymer resist films being dependent on the casting solvent and the postapplication bake temperature conditions.<sup>10</sup> In this article, we use a polymer dissolution model, based on reptation theory, in order to explain resist behavior. Experimental measurements on the dissolution of PMMA in methyl isobutyl ketone:isopropanol (MIBK:IPA) mixtures are used to test the predictions of this model.

## II. RESIST DISSOLUTION

The dissolution of high molecular weight polymer resist in an organic developer proceeds in three main stages. First, solvent from the developer penetrates the glassy polymer film forming a rubbery and swollen gel layer at the resist surface. This process is often described by case II, rather than Fickian, diffusion as a result of the strain in the gel layer due to the solvent induced swelling. Second, the stress in the gel layer relaxes by disentanglement of the polymer chains. Finally, the released and now independent polymer chains diffuse through the developer away from the developing resist surface. Each stage in the dissolution process is accompanied by a large reduction in viscosity of the polymer-solvent mixture as the solvent fraction in the polymer increases. Except with developers composed of either very

<sup>a)</sup>Author to whom all correspondence should be addressed; electronic mail: dgh4@cam.ac.uk

good or very poor solvents of the polymer, the rate limiting step is the disentanglement stage of the development. A disentanglement controlled resist dissolution process was previously described by Papanu *et al.*<sup>11</sup> who applied reptation theory<sup>12</sup> to explain a resist dissolution rate  $R$  given by

$$R = \frac{\text{thickness of monolayer}}{\tau_d}, \quad (1)$$

where  $\tau_d$  is the time taken to disentangle one polymer chain and the thickness of one monolayer was defined in terms of the radius of gyration of the polymer. The disentanglement time was derived from arguments based on the polymer self diffusion coefficient, which in turn depends on the solvent volume fraction in the resist film. In contrast to the work of Papanu *et al.*, we adopt a more direct interpretation of the monolayer thickness and reptation time. Here, we take the thickness of one monolayer to be given by the bulk density and molecular weight of the polymer and take the conventional form for the disentanglement time from the reptation theory<sup>12</sup> as

$$\tau_d = \frac{\zeta N^3 b^4}{\pi^2 k T a^2}, \quad (2)$$

where  $N$  is the number of monomers in the polymer (the polymer molecular weight  $M$  is equal to  $N$  times the monomer molecular weight  $M_m$ ),  $b$  is the monomer length,  $a$  is the lattice spacing, and  $\zeta$  is a friction term. The resist dissolution rate is then given by

$$R = \frac{\pi^2 k T M_m^3}{(\rho N_A)^{1/3} \zeta b^2 M^{8/3}}. \quad (3)$$

The friction term  $\zeta$  was modeled as an activated function with the solvent volume fraction included to account for the plasticization effect of the small solvent molecules within the polymer matrix

$$\zeta = \frac{C}{\phi^2} e^{-E_a/kT}, \quad (4)$$

where  $E_a$  is an activation energy, and  $C$  a constant depending on the nature of the polymer. The solvent volume fraction  $\phi$  is determined by consideration of the thermodynamics of the swollen gel layer. As explained by Papanu *et al.*, the energy gain by the system, through the absorption of the solvent by the polymer, is counteracted by the increase in elastic energy through swelling. An equilibrium solvent volume fraction occurs when these two energies are equal, given by the solution of the following equation:

$$0 = RT \left[ \ln(\phi) + \left(1 - \frac{V_s}{V_p}\right)(1 - \phi) + \chi(1 - \phi)^2 + V_s \rho \right. \\ \left. \times \left( \frac{2}{M_c} - \frac{1}{M} \right) \left( \frac{2}{(1 - \phi)} - 1 + \phi \right) \right], \quad (5)$$

where  $M_c$  is the critical molecular weight for the polymer and is given by the sharp increase in slope seen in viscosity versus  $M$  plots due to the onset of entanglements.  $V_s$  and  $V_p$  are the molar volumes for the solvent and polymer, respec-

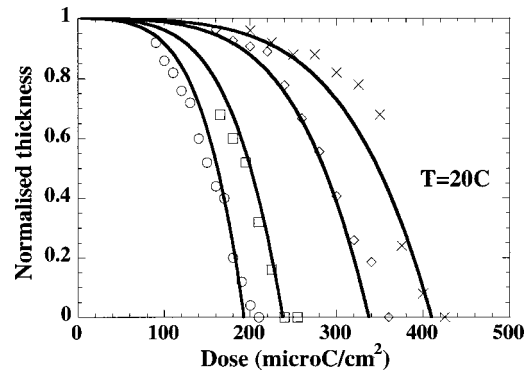


Fig. 1. Experimental contrast curves, using dip development at 20 °C, for 100 nm thick PMMA (MW 1150 K) using developer compositions of 1:1, 1:2, 1:3, and 1:4 mixtures of MIBK:IPA, respectively. Continuous curves show the model predictions using Eqs. (1)–(4). The equilibrium polymer volume fraction has been obtained from Eq. (5). The friction term has been used as a fitting parameter.

tively.  $\chi$  is the Flory interaction parameter characterizing the quality of the solvents in the developer with respect to the polymer and  $\rho$  is the bulk density of the polymer. For a given polymer, Eq. (5) predicts a range of solvent volume fractions that depend largely on the solvent quality; in the case of developer mixtures ( $\chi$  usually  $>1$ ) the solvent volume fraction is less than 0.3 and does not depend strongly on the polymer molecular weight.

### III. EXPERIMENT

Experimental contrast curves have been determined using 50 kV electron beam exposures in PMMA (MW 1150 K). Development was carried out with four different MIBK:IPA mixtures, at three different temperatures, as shown in Figs. 1, 2, and 3. The Flory interaction parameter  $\chi$  values for these developer compositions may be estimated from the solubility or cohesion parameters for PMMA, MIBK, and IPA.<sup>13</sup> Unfortunately, the literature indicates inconsistent values for these parameters so we have estimated values of  $\chi$  of 0.5 and 2 for MIBK and IPA, respectively; these values correspond to a good solvent in the first case and to a nonsolvent in the second case. These values were then used to estimate the

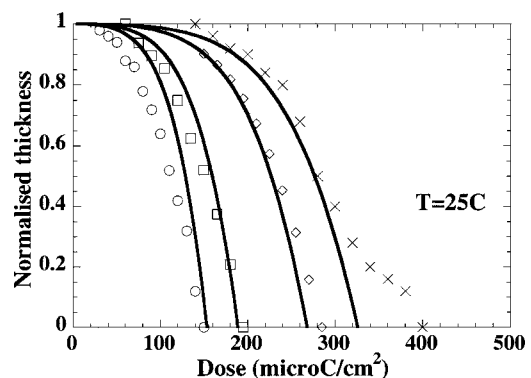


Fig. 2. As for Fig. 1, except using dip development at 25 °C.

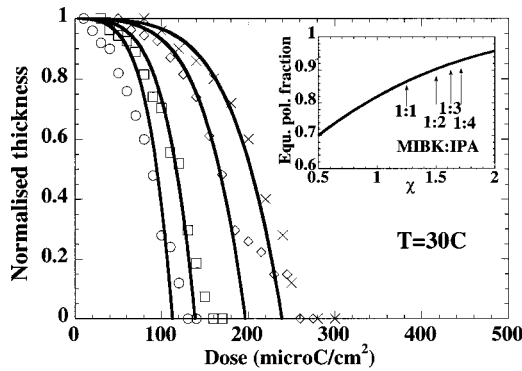


FIG. 3. As for Fig. 1, except using dip development at 30 °C. Inset: equilibrium polymer volume fraction (equal to  $1 - \phi$  neglecting the free volume) from the solution of Eq. (5) for PMMA. Solvent interaction parameter values corresponding to the developer compositions are marked by arrows.

equilibrium solvent volume fraction in the polymer for the different developer compositions based on a volume fraction weighted value for  $\chi$  in each case.

The continuous lines in Figs. 1, 2, and 3 show the model predictions, using Eqs. (1)–(4), with a correction term for resist swelling (assumed to be proportional to the equilibrium solvent concentration, given by Eq. (5) and the solution for PMMA is shown in the inset in Fig. 3). The degraded polymer molecular weight was related to the electron beam exposure dose by the equation given by Greeneich<sup>10</sup> and the parameters determined by Monte Carlo modeling. The friction term was treated as a fitting parameter giving an activation energy of about 1 eV.

Deviation of the experimental points from the predicted lines for some conditions (see Fig. 2 crosses) at doses approaching clearance may indicate phase separation which would contribute to the line edge roughness. The evolution of graininess within the developing resist is indicated in Fig. 4 where a contrast curve for a thicker layer of resist, dip developed using 1:3 MIBK:IPA at 25 °C, shows the surface

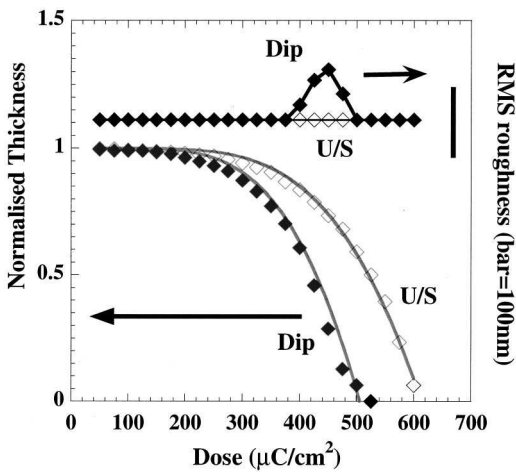
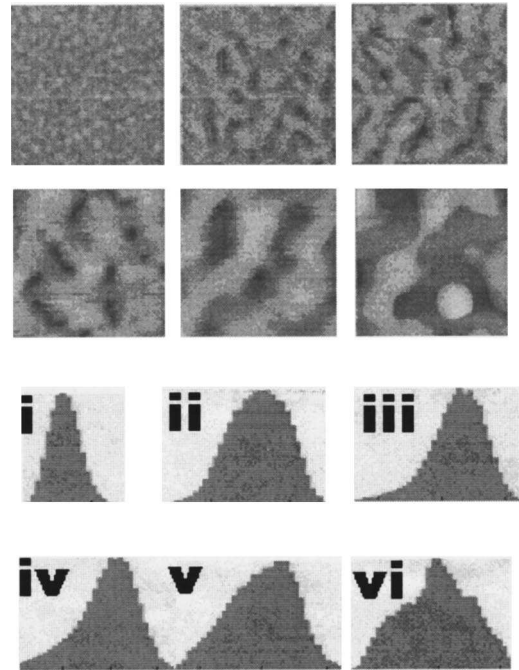
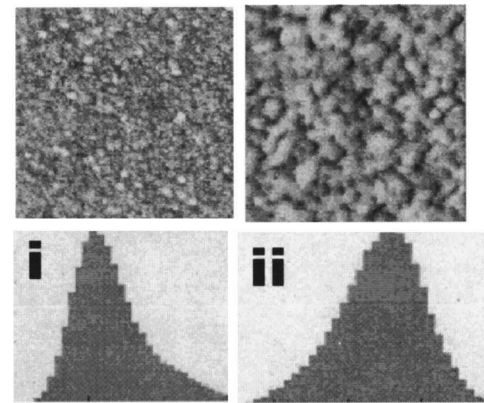


FIG. 4. Experimental contrast curves, using dip development for 30 s (♦) or ultrasonic for 5 s (◇), with 1:3 MIBK:IPA developer at 25 °C. Continuous curves show the model predictions. Also shown are the root-mean-square roughness values measured from AFM images.



(a)



(b)

FIG. 5. (a) Above AFM images ( $3 \mu\text{m} \times 3 \mu\text{m}$ ) and below: height histograms for the dip development shown in Fig. 4 for (i–vi) doses of 275 (20–40), 350 (120–210), 375 (190–290), 400 (250–370), 425 (280–520) and  $450 \mu\text{C}/\text{cm}^2$  (285–525), respectively, where the values in brackets (in nm units) indicate the histogram height range (lower and upper heights for 50% of the modal value). (b) As (a) except for the ultrasonic development shown in Fig. 4 for (i) and (ii) doses of 400 (16–32) and  $575 \mu\text{C}/\text{cm}^2$  (36–65), respectively.

roughness from atomic force microscopy (AFM) measurements. In the case of dip development, the roughness increases with dose, from the unexposed resist value, reaching a maximum slightly below the dose to clear. Island structures visible in the AFM images shown in Fig. 5, similarly increase in size with increasing dose. Histograms of the roughness indicate the appearance of two additional peaks, situated above and below the background roughness. The roughness and island size reflect the radius of gyration (dependent on the molecular weight and solvent composition of the devel-

oper), the viscosity of the developing polymer and the amount available for island formation. Samples developed with ultrasonic agitation show no change in surface roughness or appearance of island structure, see Fig. 5(b), indicating that the conditions necessary for phase separation are frustrated. Ultrasonic agitation also increases the development rate by about 3.5 times, compared to the rate for dip development at the same molecular weight, when using a power density of  $5.8 \times 10^4 \text{ W/m}^3$ . The sensitivity increases approximately linearly with ultrasonic power in this range.

#### IV. DISCUSSION

In nanolithography, the exposed lines in the resist may be of smaller width than the radius of gyration of the polymer molecules in the developer, which depends on the polymer-solvent interaction parameter  $\chi$ . In consequence, the polymer-solvent mixture inside such a narrow line may exhibit an increased viscosity, compared to the value in larger features, due to restrictions on the degrees of freedom of motion of the polymer molecule by the close proximity of the resist walls.<sup>14</sup> As a result of the increased viscosity, an increased development time is required to completely remove the exposed polymer molecule. However, as the development time is for a fixed period, it appears that an increased dose is necessary in these narrow lines for development to be completed within the time allotted. However, this additional dose increases the width of the region exposed, so that the linewidth is increased. The ultimate resolution is reached when the increase in viscosity requires an increase in dose which exactly compensates for the reduction in linewidth.

The highly concentrated polymer-solvent mixtures present during development close to the resist surface and during spin casting of the resist film, can lead to phase separation.<sup>15</sup> Solvent evaporation during spinning causes the heavier molecular weight fractions in the resist polymer to separate out preferentially as solid from the casting solvent. The radius of gyration of the polymer in the casting solvent sets the size scale for the phase separated regions leading to granularity within the resist film. During development, this phase separation may again occur. Now, the result is that the polymer rich regions, which have increased viscosity compared to the polymer poor regions, may not be removed from the developing resist before the end of the development period. If so, these regions revert to solid polymer after the post

development rinse. The size of these regions will also be determined by the radius of gyration and they will occur predominately at the edges of features. These phenomena make a significant contribution to line edge roughness.

The effect of ultrasonic agitation during development is twofold. First, a reduction in viscosity occurs due to the shear-thinning effect commonly found in polymer-solvent mixtures,<sup>15</sup> and results in more rapid development, particularly in the case of narrow features. Second, ultrasonic agitation promotes mixing through the microstreaming effect. The shorter development time and increased mixing during development inhibits the phase separation that leads to line edge roughness, and reduces the resist swelling and dose required for complete development, so improving ultimate resolution.

In conclusion, the lithographic behavior of conventional high molecular weight polymer resist may be understood with the aid of a reptation based polymer dissolution model and the solubility parameters of the developer components.

#### ACKNOWLEDGMENTS

The authors would like to acknowledge Professor Ahmed for useful discussion and the opportunity to use the fabrication facilities in the Microelectronics Research Center.

- <sup>1</sup>S. Yasin, D. G. Hasko, and H. Ahmed, *J. Vac. Sci. Technol. B* **17**, 3390 (1999).
- <sup>2</sup>K. L. Lee, J. Bucchignano, J. Gelorme, and R. Viswanathan, *J. Vac. Sci. Technol. B* **15**, 2621 (1997).
- <sup>3</sup>Shazia Yasin, A. Mumtaz, D. G. Hasko, F. Carecenac, and H. Ahmed, *Microelectron. Eng.* **53**, 471 (2000).
- <sup>4</sup>W. Chen and H. Ahmed, *Appl. Phys. Lett.* **62**, 1499 (1993).
- <sup>5</sup>M. Khoury and D. K. Ferry, *J. Vac. Sci. Technol. B* **14**, 75 (1996).
- <sup>6</sup>E. A. Dobisz, T. N. Fedynyshyn, D. Ma, L. M. Shirey, and R. Bass, *J. Vac. Sci. Technol. B* **16**, 3773 (1998).
- <sup>7</sup>T. Yamaguchi, H. Namatsu, M. Nagase, K. Yamazaki, and K. Kurihara, *Appl. Phys. Lett.* **71**, 2388 (1997).
- <sup>8</sup>E. A. Dobisz, S. L. Brandow, R. Bass, and J. Mitterender, *J. Vac. Sci. Technol. B* **18**, 107 (2000).
- <sup>9</sup>R. A. Pethrick and K. E. Rankin, *J. Mater. Chem.* **8**, 2599 (1998).
- <sup>10</sup>J. S. Greeneich, *J. Electrochem. Soc.* **122**, 970 (1975).
- <sup>11</sup>J. S. Papanu, D. S. Soane(Soong), A. T. Bell, and D. W. Hess, *J. Appl. Polym. Sci.* **38**, 859 (1989).
- <sup>12</sup>M. Doi, *Introduction to Polymer Physics* (Clarendon, Oxford, 1996).
- <sup>13</sup>A. Barton, *Handbook of Solubility Parameters and other Cohesion Parameters* (CRC Press, Cleveland, 1983).
- <sup>14</sup>K. Hagita, S. Koseki, and H. Takano, *J. Phys. Soc. Jpn.* **68**, 2144 (1999).
- <sup>15</sup>H.-G. Elias, *An Introduction to Polymer Science* (VCH, Weinheim, 1997).